15TH IEA HEAT PUMP CONFERENCE
MAY 26–29, 2026 | HOFBURG
VIENNA 2026
DECARBONISATION THROUGH INNOVATION

Experimental Evaluation of Circulation Pump Control Impact on Performance and Energy Flexibility in Heat Pumps with Thermal Storage under Rule-Based and Model Predictive Control Strategies

Maarten Evens[a,b], Alice Mugnini[c*], Alessia Arteconi[a,b]

[a]Department of Mechanical Engineering, KU Leuven 3001, Belgium
[b]EnergyVille, Genk 3600, Belgium
[c]Department of Theoretical and Applied Sciences, Università E-Campus, Novedrate 22060, Italy

Abstract

Heat pumps, often integrated with thermal energy storage, are a promising technology for efficiently meeting building heating demands while providing energy flexibility. However, assessing their operational performance and the flexibility they provide is not straightforward, as it depends on multiple factors. Notably, circulation pump control, typically integrated within the heat pump and managed by the manufacturer, is often overlooked. Since it is generally not accessible for modification, it represents a significant constraint on heat pump operation and can substantially affect overall performance. Moreover, it limits thermal storage temperatures, reducing the system ability to exploit thermal inertia and provide energy flexibility.

In this context, this study aims to experimentally assess the impact of circulation pump control on the performance and energy flexibility of a heat pump system coupled with a thermal energy storage system. The experimental setup consists of a hardware-in-the-loop configuration, in which a real water-to-water heat pump and a sensible thermal storage tank are integrated with a simulated building environment. Two different circulation pump control strategies are investigated. These strategies differ in the temperature difference imposed between the supply and return at the heat pump condenser. The impact of two high-level control strategies on system performance is evaluated: a rule-based control and a model predictive control, both tested in a laboratory setup. The predictive control is employed to activate energy flexibility, aiming to minimize electricity costs by exploiting the system thermal inertia. Results show that circulation pump control strongly influences system performance and achievable energy flexibility.

Selection and/or peer-review under the responsibility of the organizers of the 15th IEA Heat Pump Conference 2026.

Keywords: Heat Pump; Thermal Energy Storage; Energy Flexibility; Control

1. Introduction

In 2023, the residential sector accounted for 26.2% of the EU's final energy consumption, 62.5% of which was used for space heating [1], highlighting heat pumps (HPs) as a key technology for achieving the decarbonization targets of the European Green Deal [2].

The adoption of HPs enables not only efficient heat production in buildings but also, through the electrification of thermal demand, the integration of renewable energy sources and the provision of energy flexibility. This flexibility, i.e., the ability to modulate energy demand according to grid constraints or energy prices [3], can be further enhanced when HPs are coupled with thermal energy storage (TES) systems. While high-level control is often implemented using simple rule-based strategies, such as thermostats or predefined schedules, exploiting the full flexibility potential of HPs coupled with TES requires more advanced control

* Corresponding author. Tel.:
E-mail address: alice.mugnini@uniecampus.it

approaches, capable of managing key operational modes, such as compressor speed and supply temperature, according to specific objectives. Several studies have highlighted the flexibility potential of HPs combined with TES under different high-level control strategies. For example, D'Ettorre et al. [4] reported an 8% reduction in energy costs by integrating a TES into a hybrid air-source HP system under day-ahead pricing. Similarly, Li et al. [5] observed annual cost reductions up to 6.61% in a photovoltaic HP system with TES, while Péan et al. [6] achieved operational cost reductions of 1.5% in winter and up to 6.8% in summer by leveraging both the building thermal mass and a dedicated TES.

Although the studies mentioned above highlight the flexibility potential of HPs with TES, they often overlook critical onboard control strategies, such as compressor ramp rate, cycling control, auxiliary heater management, and timing constraints, as well as lower-level settings, including circulation pump control. These factors, however, significantly influence system behaviour, as demonstrated in both simulation [7] [8] and experimental studies [9] [10], and should be considered to accurately assess the achievable operational flexibility and real-world performance of HP systems.

To address these gaps, this study investigates the impact of circulation pump control on the performance and energy flexibility of a HP system. Understanding the role of circulation pump control is crucial, as most modern HPs feature integrated pumps with few adjustable parameters, and their interaction with compressor control can introduce operational uncertainties. Furthermore, when a TES is present, pump control can constrain storage temperatures, reducing the system ability to exploit thermal inertia and provide energy flexibility. In this context, several studies have demonstrated that thermal dynamics within TES significantly affect operational performance. For example, Haller et al. [11] emphasized that maintaining proper stratification is essential to optimize overall performance for both space heating (SH) and domestic hot water (DHW). Sifnaios et al. [12] further demonstrated a direct link between TES stratification and system coefficient of performance (COP), recommending tall, slim, insulated tanks with perforated plate diffusers to minimize performance losses due to flow variations. However, these studies mainly focus on optimizing the overall performance of solar thermal systems. The effect of flow variations within TES caused by internal circulation pump control strategies on the available energy flexibility and related performance remains unclear and is the focus of the present study.

To analyze this effect, experiments were conducted on a hardware-in-the-loop (HIL) setup with a water-to-water HP and a sensible hot water tank as TES, applying two different circulation pump control strategies. The strategies differ in the temperature difference imposed between the supply and return at the HP condenser. These strategies were tested under two different high-level controllers: a traditional rule-based control (RBC) and an advanced model predictive control (MPC). The MPC was selected due to its widespread use in building control, as it combines numerical optimization with feedback procedures [13]. The MPC tested in this study aims to minimize electricity costs by exploiting the thermal inertia of both the TES and the building, thereby representing a direct activation of energy flexibility. Overall, this study demonstrates that internal pump control critically influences system performance and energy flexibility, providing key insights for accurately assessing thermal-demand-driven flexibility while accounting for heat pump internal controls.

2. Methodology

This section outlines the methodology used to assess the impact of condenser-side circulation pump control on the performance and flexibility of a HP system with TES. A preliminary analysis is first conducted through exploratory charging-discharging cycles (subsection 2.1), followed by the application of two high-level control strategies: RBC (subsection 2.2) and MPC (subsection 2.3). In both cases, two condenser pump settings were tested, maintaining a temperature difference of 3 °C (ΔT3) and 10 °C (ΔT10) between supply and return. Subsection 2.4 then introduces the key performance indicators (KPIs) used to compare the outcomes. The temperature difference settings (ΔT3 and ΔT10) of the condenser pump control were selected as they represent the minimum and maximum value allowed by the manufacturer, representing the two most extreme settable operating conditions as HPs generally operate at 5 °C temperature differences.

2.1. Exploratory Charging-Discharging Cycles

To conduct a preliminary analysis of the role of circulation pump control, independently of high-level control strategies or coupling with a building, exploratory charging and discharging cycles of the TES were implemented with four distinct discharging powers. This approach fully separates the charging and discharging phases and applies fixed thermal loads, following a procedure derived from previous work [14] to evaluate the energy flexibility of a HP–TES system at nominal design capacity. As illustrated in Figure 1, the procedure considers four thermal loads distributed across four outdoor temperatures (-7 °C, 2 °C, 7 °C, and 12 °C) to account for variations in environmental conditions. For each case, the average charging and discharging times, electricity consumption, and load consumption are determined. The TES is charged from an initial temperature of 35 °C up to the maximum supply temperature setpoint of the heat pump, which is 55 °C for the unit considered in this study. The TES was considered fully discharged when the average TES temperature dropped below 35 °C

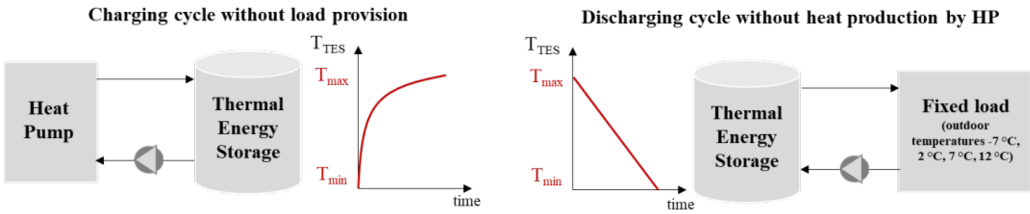

Figure 1. Procedure for carrying out separate TES charging and discharging cycles

2.2. Rule-Based Control

Unlike the approach described in the previous subsection 2.1, when a high-level control is applied, the TES–HP system is coupled with the building. Further details are provided in the following section (Section 3), where the experimental setup is described.

Regarding the RBC, the strategy does not implement any energy-flexible control and maintains the top layer of the TES within a relatively narrow range around the temperature required by the heat emission system. The hydraulic configuration of the HP–TES–building system under RBC as the high-level control is shown in Figure 2. The HP supply temperature setpoint ($T_{HP,set}$) the TES upper hysteresis ($T_{hyst,high}$), the TES lower hysteresis ($T_{hyst,low}$), and the emission system setpoint temperature ($T_{SH,set}$) are shown in Figure 3.

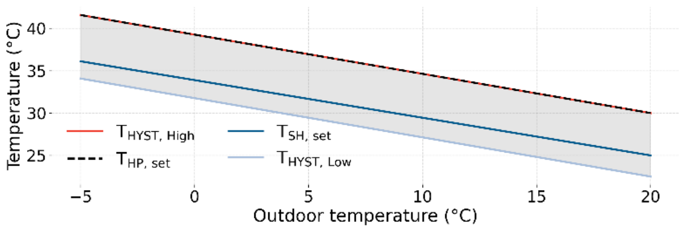

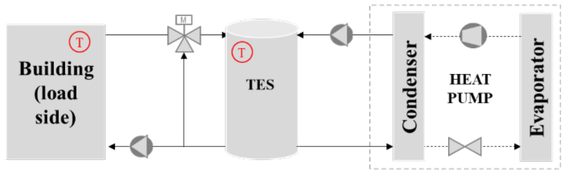

Figure 2. Hydraulic configuration of HP-TES-building with RBC as high-level control

Figure 3. Adopted heating curves on emission system ($T_{SH,set}$), HP setpoint ($T_{HP,set}$), TES charging start ($T_{hyst,low}$) and TES charging stop signal ($T_{hyst,high}$) with RBC as high-level control.

2.3. Model Predictive Control

The MPC framework consists of two main components: a predictive model and an optimization module. A comprehensive description of the control architecture is provided in the authors' previous work [15], and its implementation is available in a dedicated GitHub repository [16].

A lumped parameter model (LPM) approach is used to predict the space heating demand of a residential building with underfloor heating (archetype 3 in [15] [16]). The thermal dynamics are represented through a dual-zone configuration, modelled as a 5C8R resistive–capacitive (RC) network comprising thermal resistances (R_1–R_8), heat capacities (C_1–C_5), and key temperature states, outdoor air, envelope nodes (T_1, T_4), indoor thermal mass (T_3), and zone air temperatures (T_2, T_5). Figure 4 shows the LPM for the building. Model parameters are identified via a grey-box estimation procedure calibrated against experimental data from the real system (Section 3).

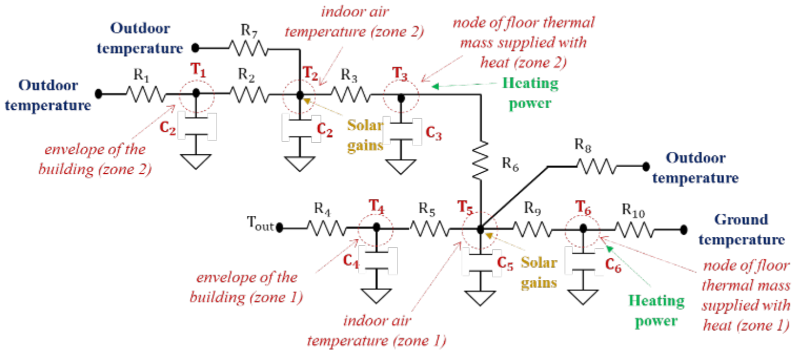

Figure 4. LPM for building with underfloor heating (archetype 3 in [15] [16])

The TES is represented by a one-dimensional stratified model, following the approach of Raccanello et al. [17]. The tank is divided into four horizontal layers of uniform thickness, each assumed to be isothermal, with the top layer. The TES model is based on an LPM structure calibrated through a grey-box identification, as detailed in Section 3. Four temperature states (T_h, T_{hm}, T_{cm}, and T_c) are defined, consistent with the methodology in [18]. Figure 5 shows the LPM for the TES**.** The estimated parameters include the thermal capacity of each layer (obtained by equally partitioning the global capacity), the heat loss coefficient, and the conductive heat transfer coefficient to the surrounding environment.

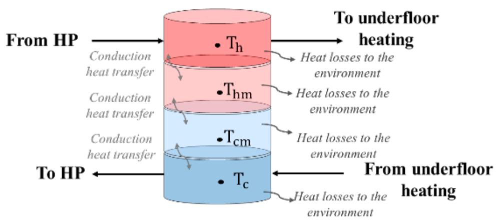

Figure 5. LPM for TES [18]

The HP is described using polynomial performance models trained on manufacturer-provided data [15]. Its operation, characterized by heating capacity and electrical power consumption, depends on the condenser outlet temperature, evaporator inlet temperature, and capacity ratio. The MPC optimizer adjusts control actions to minimize a defined objective function, in this study the electricity cost over the prediction horizon based on a given price signal, while ensuring occupant comfort and compliance with system constraints. Among the constraints is also the temperature of the hottest node of the TES; consequently, the MPC determines how and when the TES is charged. The optimization problem is solved using the IPOPT (interior point optimizer) solver via the Gekko package in Python [19]. The controller follows a receding horizon logic, meaning that at each time step the optimization is solved over a moving prediction horizon, but only the first control action is applied before the horizon shifts forward. If the MPC fails to find a feasible solution, a fallback strategy, such as a rule-based on/off controller, is employed to maintain comfort. Figure 6 illustrates the overall MPC scheme.

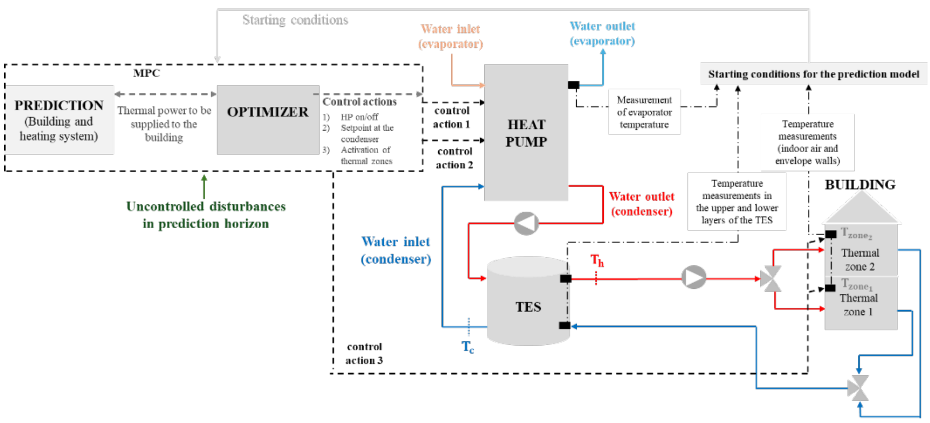

Figure 6. Schematic of the MPC application

2.4. Key Performance Indicator

The system performance was evaluated using a set of KPIs grouped into energy performance, indoor thermal comfort, flexibility, and economic impact. The following indicators were used:

Performance KPIs were used to evaluate heat pump operation and TES interaction:

- HP energy consumption (in kWh).
- coefficient of performance (COP).
- HP–load decoupling index (in %): ratio of decoupled TES usage to total TES usage; higher values indicate greater system flexibility.
- Compressor cycles.
- Average TES temperature (in °C): reflecting the overall thermal storage level and system readiness
- Average supply temperature (in °C).

Indoor comfort was assessed using indicators that capture deviations from thermostat setpoints:

- Degree-hours of discomfort when indoor temperature drops below the thermostat setpoint (in °C·h), calculated for each thermal zone to capture comfort variations.
- Degree-hours of discomfort when indoor temperature exceeds the thermostat setpoint (in °C·h), also calculated for each thermal zone.

Flexibility and TES management were evaluated through the energy flows in and out of the TES:

- Energy extracted from the TES without simultaneous HP input (in kWh), indicating how well the TES decouples generation from demand.
- Energy charged into the TES without simultaneous extraction (in kWh), assessing the system ability to preload thermal energy during off-peak hours.
- HP on-time share (%). Percentage of the total test duration during which the compressor was active.

Economic performance was evaluated based on the percentage of thermal demand covered during high-price periods relative to the total thermal demand. Therefore, when the MPC minimizes costs, the total cost is also considered a KPI.

3. Experimental set-up

The impact of the condenser circulation pump control strategy was assessed through experiments conducted using a HIL setup, from which the KPIs defined in subsection 2.4 were derived. The HIL system features a real water-to-water HP with a nominal capacity of 7.98 kW and an electricity consumption of 1.79 kW under B0/W35 conditions [20]. Further details on the measurement equipment and possible hydraulic configurations are provided in [21]. For this study, the HP was coupled with a 750-liter TES [22] to supply space heating services, as illustrated in Figure 7.

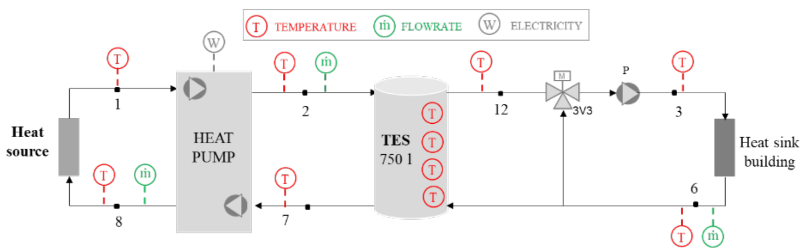

Figure 7. Hydraulic lay-out of the experimental set-up

TES temperatures were monitored at four locations evenly distributed along the tank height, while the heat source and sink were emulated via heat exchangers with controlled supply water temperature setpoints. Although the HP can provide domestic hot water, this function was disabled, as the pump control settings for domestic hot water could not be modified. Remote communication with the unit was established through a publicly available Modbus interface provided by the manufacturer [23], and experimental data were recorded at fifteen-second intervals.

As described in Section 2, to evaluate the effects of condenser pump control, two complementary approaches were employed. The first involved separate charging and discharging of the TES (subsection 2.1). The second integrated the TES with a co-simulated typical Belgian residential building, representing a two-floor, 194 m² dwelling with opaque walls and windows having thermal transmittances of 0.24 and 1.45 W/(m²·K), respectively, and a nominal heat loss of 9.4 kW at an outdoor temperature of -8 °C [8]. The building is compliant with the 2020 Flemish building regulations [24], heated by a radiant floor system. The building emulator has been developed in Modelica [8] [25]. The results of the LPM model training presented in the previous section are reported in [15] and [18].

As mentioned, two high-level control strategies were tested: RBC and MPC (subsections 2.2 and 2.3). To assess the effect of circulation pump control, two extreme condenser pump settings were applied, maintaining a temperature difference of 3 °C (ΔT3) or 10 °C (ΔT10) between supply and return, and their impact on system performance, TES stratification, and operational flexibility was evaluated. The MPC runs via two Python scripts communicating through a local database: one controls the HIL with a 15-second timestep, while the other operates the MPC with a 10-minute timestep and a 24-hour prediction horizon. The Modelica model is imported via FMPy [26], with Python as the master controller for real-time synchronization, and the HP communicates via Modbus providing measurements such as condenser temperatures and pump flow rates. Four experiments, two with RBC and two with MPC, were conducted, each lasting eight days, with the first day used to initialize the set-up and the building. The period is representative of the Belgian winter season [27]. The MPC uses a simplified daily price signal for Belgium, derived from hourly data [28]. The signal is obtained by calculating the average daily price (dark blue curve) and identifying the peak in the first half of the day (0–12 h) and the peak in the second half (12–24 h), which define the high-price periods shown as a binary signal in Figure 8. This simplified high/low price signal is used to evaluate whether the MPC can shift demand from high- to low-price periods.

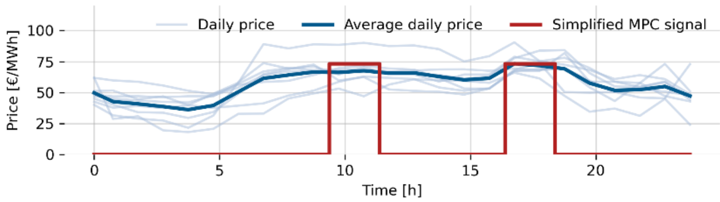

Figure 8. Price signal for MPC

4. Results

This section presents the experimental results, which are discussed in detail in Sections 4.1, 4.2, and 4.3, respectively. Section 4.1 focuses on the separated charging and discharging cycles, Section 4.2 addresses the results obtained with the RBC, and Section 4.3 presents the findings from the MPC. It should be noted that a direct comparison between RBC and MPC is not made, as the strategies operate at different TES temperature levels and follow different operational logics: RBC without considering electricity prices, MPC based on a low/high peak tariff.

4.1. Exploratory Charging-Discharging Cycles

This section presents preliminary results from HIL experimental campaigns on separated charging and discharging cycles using fixed loads, as described in subsection 2.1. The aim is to highlight, even without coupling with the building, the effect of the condenser circulation pump control.

As per procedure [14], charging the TES until the maximum achievable temperature by the HP (i.e. 55 °C in this study) was only feasible for the ΔT3 control. Figure 9 compares the charging process of the TES between the ΔT3 and ΔT10 control. As evidenced by the figure, the quick flow rate reduction for the ΔT10 control towards the end of the charging process leads to already switching off the HP at a condition where the top layers are fully charged, but the bottom layers are still up to 10 °C colder. This earlier switch-off control signal is initiated by the safety control logics of the HP in order to prevent too high condenser temperatures. In fact, Figure 9 shows that under the ΔT10 control, the pump speed is largely reduced towards the end of the charging phase in an attempt of the pump control to maintain a temperature difference of 10 °C between the condenser outlet and inlet water. This also leads to a reduced circulation in the TES and results in a larger temperature difference between the top and bottom nodes of the TES, enhancing stratification. Conversely, the ΔT3 setting produces a more mixed TES, with the lower layers being more effectively charged.

To reach successful completions of the TES charging process without activating the HP safety control logics for the ΔT10 control, the maximum TES temperature was reduced from 55 °C to 52 °C. Table 1 compares the obtained energy performance and related maximum energy flexibility potential for both condenser pump control strategies (ΔT3 versus ΔT10). Combining insights from Figure 9 with results from Table 1, it is clear that for energy flexibility services, the improved charging of the lower TES layers under the ΔT3 setting allows for greater energy storage and extends the period of self-sufficiency, during which no electricity needs to be drawn from the grid. This is reflected in the longer discharge times observed for the ΔT3 setting, as reported in Table 1. Both cases mentioned in Table 1 exploit the maximum achievable energy flexibility potential of the HP under a specific pump control strategy, i.e. charging the TES until the maximum achievable HP supply temperature of 55 °C for ΔT3 or charging until 52 °C in order to avoid activating the HP safety control logics.

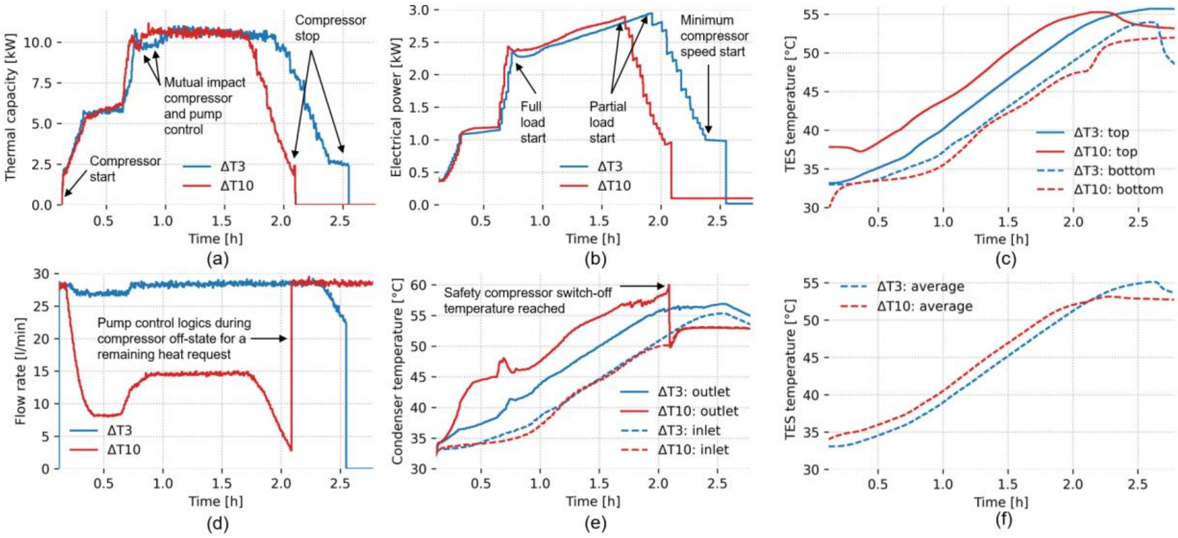

Figure 9. Comparison between ΔT3 and ΔT10 control over one, TES charging cycle when the TES is considered fully charged when an average TES temperature of 55 °C is reached. Successful completion for ΔT3 control and safety switch-off for ΔT10 control. (a): thermal capacity with indication of compressor start and stop signals. (b): electrical power consumption with indications of full and partial compressor speed conditions. (c): TES top and bottom layer temperatures. (d): condenser water flow rate with strong flow rate reductions for ΔT10 control and rather constant flow rates for ΔT3 control. (e): inlet and outlet water temperatures at the HP condenser-side with indication of compressor safety control activation for ΔT10 control. (f): average TES temperature

Table 1. Average charging and discharging time, average electricity consumption and COP for separated TES charging and discharging. Average values are reported with the associated standard deviation, calculated across different loads and ambient temperatures.

Condenser circulation pump control setting	Average charging time (hr)	Average discharging time (hr)	Average electricity consumption (kWh)	Average COP (-)
ΔT3	2.21 ± 0.004	7.15 ± 0.013	4.27 ± 0.006	3.41 ± 0.003
ΔT10	1.80 ± 0.006	6.41 ± 0.008	3.55 ± 0.005	3.67 ± 0.010

From this initial general comparison, considering only the charging and discharging cycles with fixed loads, it can be concluded that increasing the temperature difference for the condenser pump control from 3 °C to 10 °C reduces the TES energy storage potential and potentially activates the safety control logics of the HP due to too strong flow rate reductions. Finally, looking at Table 1, the ΔT3 setting obtains a lower COP than the ΔT10 setting while having a higher electricity consumption and a higher obtained average TES temperature. Other experiments at identical average TES temperatures of 52 °C were performed to evaluate if the higher COP for ΔT10 was related to the lower average TES temperature to stop charging the TES or to the improved stratification. Under all experiments, the COP at ΔT10 was higher than the COP at ΔT3, proving that higher COP at ΔT10 is obtained by an increased stratification in the TES.

4.2. Rule-Based Control

Adopting RBC with a co-simulated building, instead of separate charge and discharge cycles, Table 2 reports several KPIs described in Subsection 2.4.

It can be observed that the RBC makes limited use of the TES thermal inertia, as the decoupling index between the HP and the load remains very low. This is also related to the TES control strategy, which allows a temperature band of only 7 °C. However, the ΔT10 setting achieves a decoupling index almost four times higher. Figure 10 highlights that the significant reduction in flow rate under the ΔT10 setting causes the upper layer of the TES to reach the thermostat cut-off point, while the lower layer experiences minimal change. In contrast, the ΔT3 setting enables the HP to balance the energy supplied to the TES and the energy extracted by the load. This thermal capacity balancing allows the HP to remain in a rather continuous operation in which the TES temperature remains slightly below the TES thermostat switch-off temperature, allowing the HP to remain activated. This eventually leads to an operation where, under the ΔT3 setting, the HP closely follows the required thermal load of the building, which vanishes the energy storage potential of the TES and leads to a lower HP-load decoupling index. Although a higher energy content is also achieved with ΔT3, the TES temperature profile (see Table 2) should be considered. This indicates that ΔT10 has greater potential to decouple generation from the fulfilment of thermal demand.

Table 2. Performance, indoor comfort and flexibility and TES management KPI under RBC for ΔT3 and ΔT10 settings.

Condenser circulation pump control setting	ΔT3	ΔT10
Electricity consumption (kWh)	158.67	149.00
COP (-)	5.90	6.26
HP-load decoupling index (%)	0.26	1.03
Compressor cycles (-)	16	27
Average TES temperature (°C)	33.62	30.05
Average supply temperature (°C)	35.24	33.72
Degree-hours during which the indoor air temperature falls below 19.5 °C (sum of both floors)	3.51	3.22
Degree-hours during which the indoor air temperature exceeds 20.5 °C (sum of both floors)	1.88	1.51
Energy charged into TES without simultaneous extraction (kWh)	122.69	167.26
Energy extracted from TES without simultaneous energy input from HP [kWh]	0.26	1.03
HP on-time share (%)	66.4	67.1

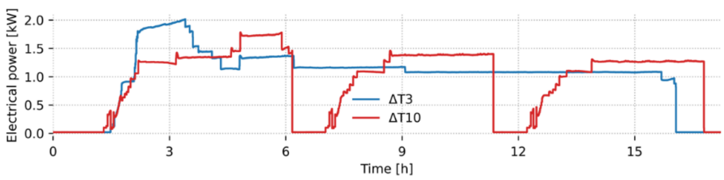

(a)

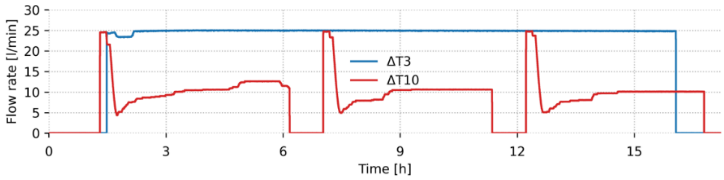

(b)

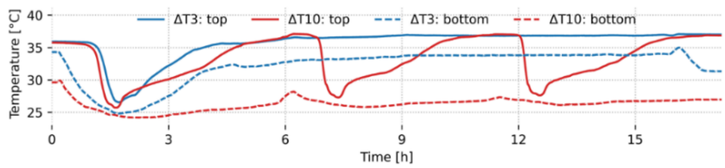

(c)

Figure 10. Comparison between ΔT3 and ΔT10 control under the RBC strategy, focusing on a representative short period of the test. ΔT3 setting reaches balance between TES energy input and output, while strong flow rate reductions for the ΔT10 setting lead to mainly charging the TES top layer and initiating HP cycling

Regarding HP performance, the lower average temperature in the condenser heat exchanger under the ΔT10 setting increases COP by 6.10% (6.26 vs. 5.90), at the expense of a 68.75% rise in compressor cycling. Considering that the RBC did not include a flexible energy management strategy, the ΔT10 setting could be recommended for normal operation due to its higher COP.

Considering thermal comfort, the ΔT10 setting achieves a slightly lower number of thermal discomfort hours. This can be explained by the fact that the strong flow rate reduction for this particular setting allows to quicker increase the supply temperature in the TES top layer when the HP is switched on. Also, switching off the HP when the TES is almost fully charged instead of attempting to match the thermal supply from the HP with the demand from the building as in the ΔT3 setting allows to slightly reduce the supply temperature to the building and to prevent overtemperatures.

A notable outcome for a ΔT10 configuration is that this control setup can potentially cause instability due to the interaction between the compressor and pump controls. Such issues are expected when the compressor speed continues to rise because the supply temperature setpoint is not reached, while the pump speed decreases due to a low temperature difference between supply and return water. The magnitude of each control action is therefore critical. However, no instability was observed in the experiments, thanks to the large 750 l TES, which allows the compressor to accelerate before the pump slows significantly. Preliminary tests including domestic hot water showed instability when switching between services. In these cases, the TES was partially charged for space heating, and pump control caused rapid flow reductions before the slower compressor controller could respond, leading to unnecessary compressor cycling. For the present study, focusing on space heating only, such oscillations did not occur. This highlights the need to carefully consider potential cross-interactions between compressor and pump control during both system design and heat pump parameterization.

4.3. Model Predictive Control

This section analyses the results of applying MPC to a co-simulated building, with several KPIs reported in Table 3 (see Subsection 2.4). Overall, the MPC is highly effective: in the ΔT3 scenario, the RBC backup was needed for only 1.83 h, allowing 99% autonomous operation, while in ΔT10 it was required for 3.17 h, corresponding to 98.3% autonomous operation.

Comparing the condenser circulation pump control strategies ΔT3 and ΔT10, several differences emerge relative to the results observed under RBC (Subsection 4.2). In terms of energy performance, electricity consumption is significantly lower with ΔT3 (184.93 kWh vs. 244.97 kWh, a 24.5% reduction), accompanied by a higher COP (5.50 vs. 4.18, a 31.6% increase), indicating more efficient system operation. Compressor cycling is reduced with ΔT3 (102 vs. 132), while HP on-time is higher (84.4 % vs 72.9 %), resulting in fewer but longer compressor cycles, which can improve reliability and reduce equipment wear.

Although ΔT3 achieves better operational performance than ΔT10, it is important to emphasize that the primary goal of MPC is not simply to minimize energy consumption, but to leverage system flexibility and reduce electricity costs. From this flexibility perspective, ΔT10 performs better. The pump load decoupling index is lower with ΔT3 (31.11 %) than with ΔT10 (50.22 %), meaning that ΔT10 achieves greater decoupling between thermal demand and generation. Similarly, TES management is more flexible with ΔT10. Specifically, the energy charged without simultaneous extraction is higher with ΔT10 (513.85 kWh) than with ΔT3 (316.31 kWh), and the energy extracted without concurrent HP input is also higher with ΔT10 (193.73 kWh vs. 130.4 kWh for ΔT3). Moreover, the average TES and supply temperatures are higher with ΔT10. In particular, the average TES temperature increases from 36.46 °C in the ΔT3 case to 43.46 °C in the ΔT10 case, an increase of 19.2 %, while the average supply temperature rises from 37.71 °C to 46.4 °C, an increase of 23.1 %. These differences explain the observed performance, showing that with MPC ΔT10 the system achieves a larger effective storage capacity and better exploitation of thermal flexibility.

Table 3. Performance, indoor comfort and flexibility and TES management KPI under MPC for ΔT3 and ΔT10 settings.

Condenser circulation pump control setting	ΔT3	ΔT10
Electricity consumption (kWh)	184.93	244.97
COP (-)	5.50	4.18
HP-load decoupling index (%)	31.11	50.22
Compressor cycles (-)	102	132
Average TES temperature (°C)	36.46	43.46
Average supply temperature (°C)	37.71	46.4
Degree-hours during which the indoor air temperature falls below 19.5 °C (sum of both floors)	2.83	2.32
Degree-hours during which the indoor air temperature exceeds 20.5 °C (sum of both floors)	37.37	102.18
Energy charged into TES without simultaneous extraction (kWh)	316.31	513.85
Energy extracted from TES without simultaneous energy input from HP [kWh]	130.4	193.73
HP on-time share (%)	84.4	72.9
Share of thermal demand at high prices (%)	15.0	14.30

Regarding thermal comfort, ΔT3 exhibits slightly more hours below 19.5 °C (2.83 h vs. 2.32 h), while hours above 20.5 °C are substantially lower (37.37 h vs. 102.18 h), indicating better overheating management with ΔT3. Overall, these differences are primarily due to the predictive model slightly underestimating the indoor temperature. This is illustrated in Figure 11, which provides a detailed example of predicted versus measured temperatures in the two thermal zones for ΔT10 throughout the experiment. Nevertheless, the predictive performance remains quite good, with the average Root Mean Square Error between zones below 1 °C (0.57 °C for ΔT3 and 0.67 °C for ΔT10).

Finally, the share of thermal demand satisfied during high-price periods is slightly higher with ΔT3 (15 % vs 14.3 %). Nonetheless, this does not contradict the superior load-shifting capability of ΔT10, which more effectively reschedules consumption to align with high-price periods.

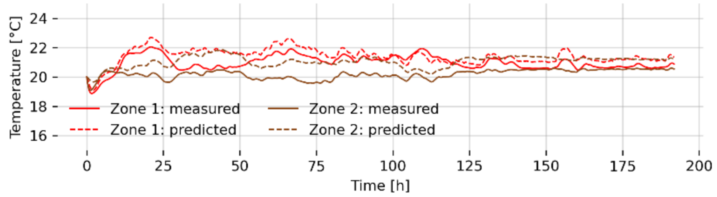

Figure 11. Comparison of predicted and measured temperatures in the two thermal zones for the ΔT10 scenario over the entire duration of the experiment

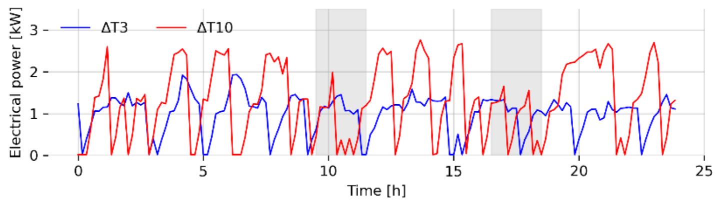

(a)

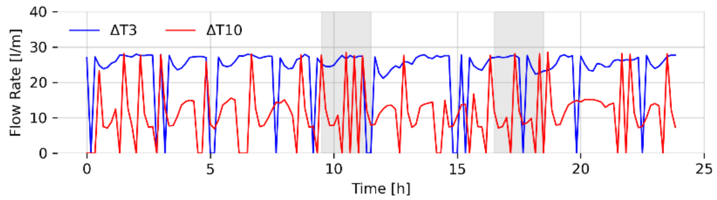

(b)

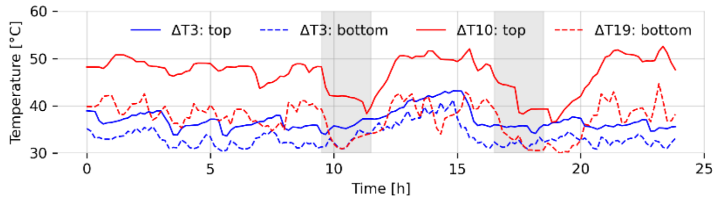

(c)

Figure 12. Comparison of ΔT3 and ΔT10 control under the MPC strategy, focusing on a representative short period of the test: (a) electricity consumption, (b) condenser-side mass flow rate, and (c) TES temperature. Shaded gray areas indicate high-price periods

In summary, ΔT10 under MPC provides superior flexibility, enabling greater load shifting towards high-price periods, as also evidenced by the dynamic variables shown in Figure 12. Conversely, ΔT3 ensures better performance in terms of energy efficiency and COP. However, it is important to emphasize that the differences observed in KPI values between the tests conducted with RBC and MPC are attributable to the different average and maximum TES temperatures (Tables 2 and 3). These variations stem from the way the high-level control operates, with RBC being constrained by the setpoint according to a heating curve with a 30 – 42 °C range, whereas in the case of the MPC, the behaviour of the system is determined by the optimizer, which can set the supply temperature (which is a decision variable) to any value between 25 °C and 55 °C, representing the allowable minimum and maximum limits, respectively. Therefore, a direct comparison of KPI values between the two high-level controllers is not meaningful. Nevertheless, examining their performance in conjunction with the two different circulation pump settings remains valuable, as it highlights the distinct behaviours induced by the control for a given high-level controller.

5. Conclusions

This study investigates the impact of condenser circulation pump control on the performance and energy flexibility of a water-to-water heat pump system coupled with a thermal energy storage unit. Low-level pump control strategies are often embedded within the heat pump by the manufacturer and may be protected, yet their influence on building-integrated operation is rarely assessed. To address this, experiments were conducted using a hardware-in-the-loop setup combining a real heat pump with a simulated building environment. Two circulation pump control strategies were adopted, maintaining either a 3 °C (ΔT3) or 10 °C (ΔT10) temperature difference between the supply and return water at the condenser. The analysis considered both isolated thermal energy storage charging and discharging cycles with fixed loads, to evaluate storage behavior independently of the building load, and coupled operation with the simulated building under two high-level control schemes: rule-based control and model predictive control.

Under fixed-load tests, the ΔT10 strategy, characterized by a higher temperature difference across the condenser, produced stronger stratification in the thermal energy storage unit but reduced the total charging capability compared to the ΔT3 strategy, which maintained a more mixed storage tank. During coupled operation under rule-based control, ΔT10 achieved a decoupling index (defined as the fraction of thermal energy storage energy used independently of heat pump operation) almost four times higher than ΔT3, demonstrating superior potential for energy flexibility. In contrast, ΔT3 ensured better thermal balance between the heat pump and the building load, resulting in greater overall stored energy and fewer compressor cycles, which may reduce equipment wear. However, ΔT10 may introduce instabilities between compressor and pump control when the flow rate is strongly reduced to achieve the 10 °C setpoint while the compressor ramps up.

When operating under model predictive control, the differences between the two pump strategies became more pronounced. ΔT3 led to lower electricity consumption and a higher coefficient of performance, reflecting more efficient operation. Conversely, ΔT10 enhanced energy flexibility, achieving higher decoupling indices and larger amounts of energy charged and discharged independently of heat pump activity, enabling more effective load shifting toward high-price periods.

These findings highlight the crucial role of circulation pump control in balancing energy efficiency, system flexibility, and equipment reliability. Future work will focus on extending the analysis to multi-service operation and exploring the dynamic interactions between compressor and pump control under varying conditions.

References

[1] Eurostat. Available online: ec.europa.eu/eurostat/databrowser/view/nrg_d_hhq/default/table?lang=en (Verified access on October 24, 2025)
[2] European Commission, 2019. The European Green Deal (COM(2019) 640 final).
[3] Jensen S.Ø., Marszal-Pomianowska A., Lollini R., Pasut W., Knotzer A., Engelmann P., Stafford A., Reynders G., 2017. “IEA EBC Annex 67 Energy Flexible Buildings”, *Energy and Buildings*, Volume 155, 2017, Pages 25–34, doi.org/10.1016/j.enbuild.2017.08.044
[4] D’Ettorre F., De Rosa M., Conti P., Testi D., Finn D., 2019. “Mapping the energy flexibility potential of single buildings equipped with optimally-controlled heat pump, gas boilers and thermal storage”, *Sustainable Cities and Society*, Volume 50, 2019, 101689, doi.org/10.1016/j.scs.2019.101689
[5] Li B., Liu Z., Zheng Y., Xie H., Zhang L., 2024. “Economy and energy flexibility optimization of the photovoltaic heat pump system with thermal energy storage”, *Journal of Energy Storage*, Volume 100, Part A, 2024, 113526, doi.org/10.1016/j.est.2024.113526
[6] Péan T., Costa-Castelló R., Fuentes E., Salom J., 2019. “Experimental testing of variable speed heat pump control strategies for enhancing energy flexibility in buildings”, *IEEE Access*, Volume 7, 2019, ieeexplore.ieee.org/document/8674547#citations
[7] Clauß J., Georges L., 2019. “Model complexity of heat pump systems to investigate the building energy flexibility and guidelines for model implementation”, *Applied Energy*, Volume 255, 2019, 113889, doi.org/10.1016/j.apenergy.2019.113889

[8] Evens M., Arteconi A., 2021. “Influence of internal control simplifications in heat pump system modelling for energy flexibility evaluations”, *Proceedings of Building Simulation 2021: 17th Conference of IBPSA*, 2021, Pages 1212–1219, doi.org/10.26868/25222708.2021.30214
[9] Finck C., Li R., Zeiler W., 2020. “Optimal control of demand flexibility under real-time pricing for heating systems in buildings: A real-life demonstration”, *Applied Energy*, Volume 263, 2020, 114671, doi.org/10.1016/j.apenergy.2020.114671
[10] Evens M., Arteconi A., 2024. “Design energy flexibility within a comfort and climate box – An experimental evaluation of the internal heat pump control effects”, *Applied Thermal Engineering*, Volume 254, 2024, 123842, doi.org/10.1016/j.applthermaleng.2024.123842
[11] Haller M.Y., Haberl R., Reber A., 2019. “Stratification efficiency of thermal energy storage systems – A new KPI based on dynamic hardware in the loop testing - Part II: Test results”, *Energy and Buildings*, Volume 202, 2019, 109366, doi.org/10.1016/j.enbuild.2019.109366
[12] Sifnaios I., Fan J., Olsen L., Madsen C., Furbo S., 2019. “Optimization of the coefficient of performance of a heat pump with an integrated storage tank – A computational fluid dynamics study”, *Applied Thermal Engineering*, Volume 160, 2019, 114014, doi.org/10.1016/j.applthermaleng.2019.114014
[13] Serale G., Fiorentini M., Capozzoli A., Bernardini D., Bemporad A., 2018. “Model predictive control (MPC) for enhancing building and HVAC system energy efficiency: Problem formulation, applications and opportunities”, *Energies*, Volume 11, 2018, 631, doi.org/10.3390/en11030631
[14] Evens M., Mugnini A., Arteconi A., 2022. “Design energy flexibility characterisation of a heat pump and thermal energy storage in a Comfort and Climate Box”, *Applied Thermal Engineering*, Volume 216, 119154, doi.org/10.1016/j.applthermaleng.2022.119154
[15] Mugnini A., Evens M., Arteconi A., “Model predictive controls for residential buildings with heat pumps: Experimentally validated archetypes to simplify the large-scale application”, *Energy and Buildings*, Volume 320, 2024, 114632, doi.org/10.1016/j.enbuild.2024.114632
[16] GitHub repository for MPC archetypes: github.com/diismunivpm/PredictiveArchHP
[17] Raccanello J., Rech S., Lazzaretto A., 2019. “Simplified dynamic modeling of single-tank thermal energy storage systems”, *Energy*, Volume 182, Pages 1154-1172, doi.org/10.1016/j.energy.2019.06.088
[18] Mugnini A., Evens M., Felicetti R., Ferracuti F., Arteconi A., “Experimental analysis on the role of modeling sensible Thermal Energy Storages in Model Predictive Controls applied to buildings with Heat Pumps”, *REHVA HVAC World Congress CLIMA 2025*.
[19] Beal et al., "GEKKO Optimization Suite," Processes, vol. 6, no. 8, 2018. doi.org/10.3390/pr6080106
[20] Daikin, "Geothermal HP EGSAX06D9W," 2020
[21] Clima2022 paper
[22] Viessmann, "Vitocell 100-E Technical Specifications," 2019
[23] DCOM LT IO MB
[24] Flemish Energy Agency (VEA), “EPB-eisen vanaf 1 januari 2020 tot en met 31 december 2020,” 2020.
[25] Jorissen F., Reynders G., Baetens R., Picard D., Saelens D., and Helsen L., “Implementation and verification of the IDEAS building energy simulation library,” J. Build. Perform. Simul., vol. 11, no. 6, pp. 669–688, 2018, doi: 10.1080/19401493.2018.1428361.
[26] FMPy,” Dassault Systèmes.
[27] Evens M., Arteconi A., 2023 “Representative cycle for heat pump energy flexibility evaluations – A comparative simulation study of existing day selection procedures to a new consecutive day procedure”, *Energy and Buildings*, Volume 297, 2023, doi.org/10.1016/j.enbuild.2023.113443
[28] Elexys, “Belgian Day-Ahead electricity prices,” Elexys.